Received: Added at production | Revised: Added at production | Accepted: Added at production

DOI: xxx/xxxx

RESEARCH ARTICLE

Multi-Variable and Multi-Objective Gain-Scheduled Control Based on Youla-Kucera Parameterization: Application to Autonomous Vehicles

Hussam Atoui*[1,2] | Olivier Sename[2] | Vicente Milanes[3] | John-Jairo Martinez-Molina[2]

[1]Research Department, Renault SAS, Guyancourt, France
[2]Control Department, Univ. Grenoble Alpes, CNRS, Grenoble INP, GIPSA-lab, Grenoble, France
[3]Spanish Engineering Division, Renault España SA, Valladolid, Spain

Correspondence
*Hussam Atoui, 1 Avenue de Golf, 78280 Guyancourt, France. Email: hussam.atoui@outlook.com

Present Address
1 Avenue de Golf, 78280 Guyancourt, France

Abstract

This paper presents a Youla-Kucera based interpolation between a set of Linear Parameter-Varying (LPV) controllers, each one being a gain-scheduled of Linear Time-Invariant (LTI) controllers designed separately for different operating points. The gain-scheduling is achieved based on Youla-Kucera (YK) parameterization. A generalized LPV-YK control structure is designed to interpolate between various LPV controllers. The closed-loop system is proved to guarantee the quadratic stability for any continuous/discontinuous interpolating signals in terms of a set of Linear Matrix Inequalities (LMIs). The proposed method can help multi-variable and multi-objective systems to achieve high performances at different operating conditions and different critical situations regardless of the interpolation rate. A numerical example is simulated to show the importance of the proposed method to achieve different objectives for lateral control of autonomous vehicles. In addition, the approach has been tested on a real Renault ZOE vehicle to validate its real performance, and compare it with a standard polytopic LPV controller.

KEYWORDS:
Youla Parameterization, LPV Control, Autonomous Vehicles, Multi-objective Systems

1 Introduction And Motivation

Nowadays, systems are getting more and more complex leading to control algorithms able to consider online varying objectives for performance and safety. The field of autonomous systems, in particular autonomous vehicles, is indicative of such an evolution. Indeed, their driving capabilities have been recently improved for highly, and even fully, autonomous driving thanks to advanced control theory. A fully autonomous car needs to perform several tasks including longitudinal control, lateral control, chassis control, etc. Moreover, the lateral dynamics of an autonomous vehicle varies significantly with respect to its longitudinal speed[1,2]. Specifically, at low speeds, the lateral dynamics becomes harder to be controlled (due to approaching system singularity), whereas at high speeds, robustness and system stability decrease[3]. On the other hand, even at nominal speeds, the lateral control aims to achieve various objectives such as lane tracking, lane changing, obstacle avoidance, etc. Consequently, various performances are required accordingly for different traffic situations that faces the vehicle. However, it is difficult to design a single controller covering the full speed range and achieving multiple objectives. As shown below, some solutions have been investigated in the literature to design multi-variable and multi-objective controllers to obtain various closed-loop performances.

1.1 Gain-scheduling Control Systems

In the last decades, research studies have developed multi-variable control systems using gain-scheduling techniques, see for instance the pioneering works[4,5]. Gain-scheduling controls are used when a plant changes significantly within its operating conditions; which is actually the case in many real applications, see[6] and references therein. For time-varying systems, it may not possible to find a single Linear Time-Invariant (LTI) controller that can perform well for all operating conditions. Therefore, the Linear Parameter-Varying (LPV) control concept has been successfully developed to achieve a stable gain-scheduling[7], self-scheduling[8] or interpolation[9] between LTI systems synthesized at different operating points.

LPV control design methods have been examined with successful control applications on autonomous vehicles, see for instance[10,11,12] and references therein. Nonetheless, it is today admitted that designing a single LPV controller for a large number of parameters, and/or for a wide range of variations of parameters may be conservative[13]. Two main solutions could be used to decrease the optimization problem conservatism: 1) Divide the parameter region into small subregions and use multiple parameter-dependent Lyapunov functions[13]; and 2) Use the Youla-Kucera (YK) parameterization to interpolate between different LTI controllers designed separately at each operating condition[14].

The interest behind YK concept is to parameterize a set of linear stabilizing controllers $K(Q)$ where each one is parameterized by its corresponding YK parameter Q[15]. In[16], a YK configuration is considered to improve the performance of a polytopic LPV control. It introduces an LPV system which switches between a minimum-phase and nonminimum-phase dynamics as a function of the parameter variations. An LPV controller based on the polytopic approach is designed as a nominal controller in the full parameter region. Then, two different LTI controllers ($\mathcal{H}_\infty$ and PID) are designed separately at certain operating conditions (one in minimum-phase region and another in nonminimum-phase region). These LTI controllers are then interpolated with the nominal LPV controller using an LTI-YK configuration.

On the other hand,[14] proposes a YK-based gain-scheduled controller by interpolating LTI controllers designed separately at the different vertices of a polytopic parameter region. The interpolation is performed as a function of the varying parameters of the LPV model. Closed-loop quadratic stability and performance are guaranteed at intermediate interpolation points of the convex domain. In[17], a fixed pole-assignment application is introduced using an LPV YK-based method to preserve the closed-loop poles at the same location by interpolating between different controllers.

In[18] an observer-based state-feedback LPV controller is designed based on Youla parameterization. It is proved that any quadratically stabilizing LPV controller can be parameterized based on YK concept, providing the closed-loop quadratic stability. A parameter-varying YK parameter $Q(\rho)$ is designed, being ρ a measurable varying parameter.

1.2 Youla-Kucera for Multi-Objective Control Systems

In addition to parameter-varying control performance, it may be required to reach several performance specifications (high robustness, fast/slow response, noise rejection, etc.) at each operating condition of the varying parameter region. The YK configuration has been widely used to interpolate between different performances, however mainly for LTI systems. Hespanha and Morse[19] propose the YK concept to interpolate between two LTI controllers (slow and fast) to handle both noise rejection and fast tracking performances.

The YK parameterization for interpolating controllers has shown several advantages: 1) It allows stable interpolation between unstable controllers[20]; 2) Interpolated controllers can be designed and tuned separately using different techniques ($\mathcal{H}_\infty$, LQR, PID, ...)[21]; 3) It facilitates adding new parts to an existing system online as Plug&Play control theory[22]; and 4) The closed-loop stability is guaranteed under arbitrary continuous/discontinuous interpolating signals between different stabilizing controllers without requiring a common Lyapunov function[19].

Recently, [23] proposes a YK-based interpolation scheme between two LPV controllers, designed separately, to achieve a multi-objective control system. Each LPV controller is designed over a convex domain with a common Lyapunov function (following the approach in [8]), to quadratically stabilize the plant model. However, this approach may be conservative since it requires all the local LPV controllers to be designed based on standard polytopic-based LPV approach.

A significant literature review on YK work including applications can be found in[23]. The YK parameterization has been successfully used in several domains such as noise/vibration control[24], and steering control of autonomous vehicles considering two LTI controllers designed separately (one for lane-changing and one for lane-tracking)[25]. The YK control scheme of both controllers has shown interesting performance for small and large lateral errors. On the other hand, the YK controller is parameterized for a fixed-speed (LTI lateral dynamics). Our paper proposes a generalized LPV-YK control structure that interpolates between multiple LPV controllers obtaining a multi-variable and multi-objective gain-scheduled controller.

1.3 Motivation and Contribution

Apart from the YK concept, there has been a wide range of research to develop an LPV switching controller (see for instance [13,26]). Recent extensions have mainly aimed to decrease the design complexity and conservatism [27], and to provide smooth switching [28]. However, the LPV switching studies are still conservative due to the re-design of the local LPV controllers by proposed LMIs, in addition to some limitations that restrict the switching signals (e.g. hysteresis switching, switching with average dwell-time, etc.). The current work proposes an LPV interpolation/switching control scheme with lower conservatism and without any limitation on the switching signals. A new survey about different LPV switching methods, including YK-based approach, is presented in [29].

A main motivation behind considering an interpolation scheme between multiple LPV controllers is the application to autonomous vehicles. Several studies have involved the LPV control approaches to solve the lateral tracking problem over the full speed-range (speed as the varying parameter), such as LPV/LFT [11] and grid-based LPV [12,30]. However, it is not sufficient to achieve several tracking performances (e.g. smooth and aggressive). On the other hand, [25] has integrated lane-tracking and lane-changing control performances at a constant speed using LTI-YK concept.

Our work proposes a generalized LPV-YK control configuration which can guarantee several control objectives over the full speed-range. The main contributions are as follows:

1. An interpolation scheme of multiple LPV controllers is designed based on YK concept. Such scheme is considered to be more efficient and less conservative than the LPV switching control systems where: 1) There is no limitation on the switching/interpolating signals; 2) The local LPV controllers are designed based on LTI-YK parameterized controllers; 3) All the local LPV and LTI controllers are pre-defined and designed separately without requiring any common condition or re-design.

2. A generalized LPV-YK interpolation scheme is defined and proved to achieve closed-loop quadratic stability with smooth assumptions and LMI conditions.

3. A significant simulation shows the importance of the proposed LPV-YK control structure in improving the performance of the autonomous vehicles in various tasks and critical situations.

4. For the first time, the LPV-YK control scheme is implemented on a real Renault ZOE vehicle. An experimental test on the vehicle lateral control enhances the stability of the closed-loop system at the interpolating time instants, and shows the different performances achieved by the vehicle.

As a result, an interpolation scheme is drawn between multi-LPV controllers based on YK parameterization which guarantees the closed-loop quadratic stability under arbitrary interpolating signal. Moreover, it shows high flexibility to achieve various performance levels, and to add or remove controllers from the interpolation scheme without repeating the design step.

The paper is organized as follows: Section 2 defines the YK concept with some Lemmas to be used throughout the paper. The problem statement is expressed in Section 3. Section 4 introduces the main results, including the quadratic stability analysis. Section 5 presents the implementation control scheme of the LPV-YK controller. Section 6 shows an application to the autonomous vehicle lateral control, including simulation results. Experimental results of a robotized Renault ZOE vehicle are depicted in Section 7. Finally, some concluding remarks are given in Section 8.

Notations in this paper are as follows. $\mathbb{I}[a, b]$ denotes the integer set from a to b. $\mathbb{R}$ stands for the set of real numbers. $\mathbb{R}^{m\times n}$ is the set of real $m \times n$ matrices. The transpose of a real matrix M is denoted by M^T. I and 0 denote an identity matrix and a zero matrix, respectively, of appropriate dimensions. $diag(X_1, X_2, ..., X_N)$ denotes a matrix with matrices X_1, X_2, ..., and X_N as diagonal blocks. Define a vector $\gamma = [\gamma_1 \dots \gamma_\zeta]$, we note by $\gamma_c^* = 1$ if $\gamma_c = 1$ and $\gamma_j = 0\ \forall j \neq c$.
In the whole paper, the subscript i of a system/matrix/variable of an LPV system (e.g. G_i, A_i, w_i) denotes the local LTI system/-matrix/variable at the i^{th} vertex of a polytope $\mathcal{P}$. The superscript (j) denotes the j^{th} controller (e.g. $K^{(j)}$) in the set of designed controllers. For example, $A_{k,i}^{(j)}$ represents the state matrix of the j^{th} LTI local controller at the i^{th} vertex of $\mathcal{P}$.

2 Preliminaries

This section introduces some notations and assumptions regarding LPV systems and LTI-YK parameterization. In addition, useful concepts and several lemmas are reviewed.

2.1 State Transformation

The concept of state transformation is to evolve the states of a system without affecting its input/output property. Consider a state transformation matrix T which transforms the state of a dynamic system W with the state-space representation; $W : \left[\begin{array}{c|c} A & B \\ \hline C & D \end{array}\right]$. Then, the transformed system $\bar{W}$ is computed as:

$$\bar{W} : \left[\begin{array}{c|c} TAT^{-1} & TB \\ \hline CT^{-1} & D \end{array}\right]. \tag{1}$$

Lemma 1. Consider a set of matrices A_i corresponding to each vertex of a convex hull $\mathcal{J} = \mathcal{C}_{\mathcal{O}}\{w_1, ..., w_{2^{n_p}}\}$, The following statements are equivalent:

(i) A_i is Hurwitz $\forall i \in \mathbb{I}[1, 2^{n_p}]$

(ii) there exist 2^{n_p} transformation matrices T_i such that the LPV matrix

$$\bar{A}(\rho) = \sum_{i=1}^{2^{n_p}} \alpha_i(\rho)\bar{A}_i = \sum_{i=1}^{2^{n_p}} \alpha_i(\rho)T_iA_iT_i^{-1} \tag{2}$$

is quadratically stable $\forall \rho \in \mathcal{J}$, where $\rho = \sum_{i=1}^{2^{n_p}} \alpha_i(\rho)w_i$ such that $\sum_{i=1}^{2^{n_p}} \alpha_i(\rho) = 1$, $\alpha_i(\rho) \geq 0 \; \forall i$.

Proof details are in [14] and [19].

2.2 Doubly Coprime Factorisation

YK parameterisation uses the doubly coprime factorisation concepts to reduce the algebraic complexity of Q computation [31]. Let K be an LTI controller that stabilizes the LTI plant G, then both of them can be factorized (from left and right) as a product of a stable transfer function matrix and a transfer function matrix with a stable inverse as shown below:

$$\begin{aligned} G &= NM^{-1} = \tilde{M}^{-1}\tilde{N} \\ K &= UV^{-1} = \tilde{V}^{-1}\tilde{U} \end{aligned} \tag{3}$$

Lemma 2. If the coprime factors $M, N, \tilde{M}, \tilde{N}, U, V, \tilde{U}, \tilde{V} \in \mathcal{RH}_\infty$ (proper, stable and rational), and they satisfy the following *Bezout Identity*:

$$\begin{aligned} \begin{bmatrix} \tilde{V} & -\tilde{U} \\ -\tilde{N} & \tilde{M} \end{bmatrix} \begin{bmatrix} M & U \\ N & V \end{bmatrix} &= \begin{bmatrix} M & U \\ N & V \end{bmatrix} \begin{bmatrix} \tilde{V} & -\tilde{U} \\ -\tilde{N} & \tilde{M} \end{bmatrix} \\ &= \begin{bmatrix} I & 0 \\ 0 & I \end{bmatrix} \end{aligned} \tag{4}$$

then, the factorized LTI controller $K = UV^{-1}$ stabilizes G [21].

2.3 Interpolation of two LPV controllers based on LPV-YK parameterization

This section summarizes some results already presented by the authors in [32]. Assume a set of two LPV controllers $\{K^{(0)}(\rho), \; K^{(1)}(\rho)\}$ that have been designed separately to quadratically stabilize an LPV plant $G(\rho)$ over a convex parameter region $\mathcal{P}$ ($\rho \in \mathcal{P}$). Let us choose $K^{(0)}(\rho)$ as the nominal controller for YK parameterization. Denote the LPV-YK parameter $Q^{(1)}(\rho)$ as a transfer function matrix which characterizes the dynamic variation between $K^{(0)}(\rho)$ and its corresponding controller $K^{(1)}(\rho)$.

Lemma 3. Assume a factorized LPV plant $G(\rho) = N(\rho)M^{-1}(\rho)$, and factorized LPV controllers $K^{(0)}(\rho) = U^{(0)}(\rho)(V^{(0)}(\rho))^{-1}$ and $K^{(1)}(\rho) = U^{(1)}(\rho)(V^{(1)}(\rho))^{-1}$ that quadratically stabilize $G(\rho)$ over $\mathcal{P}$, with $M(\rho)$ and $N(\rho)$ are parameter-varying, coprime and stable, $U^{(0)}(\rho)$ and $V^{(0)}(\rho)$, $U^{(1)}(\rho)$ and $V^{(1)}(\rho)$ are parameter-varying, coprime and stable. Choosing $K^{(0)}(\rho)$ as the nominal controller, then, the interpolation between both LPV controllers $K^{(0)}(\rho)$ and $K^{(1)}(\rho)$ can be performed using the parameterized

LPV-YK controller $\tilde{K}^{(1)}(\rho,\gamma)$ defined as:

$$\begin{aligned}\tilde{K}^{(1)}(\rho,\gamma) &= \Big(U^{(0)}(\rho) + M(\rho)\gamma Q^{(1)}(\rho)\Big)\Big(V^{(0)}(\rho) + N(\rho)\gamma Q^{(1)}(\rho)\Big)^{-1} \\ &= \Big(\tilde{V}^{(0)}(\rho) + \gamma Q^{(1)}(\rho)\tilde{N}(\rho)\Big)^{-1}\Big(\tilde{U}^{(0)}(\rho) + \gamma Q^{(1)}(\rho)\tilde{M}(\rho)\Big)\end{aligned} \tag{5}$$

where $\gamma \in [0,1]$ is the interpolating signal. Notice that $K^{(0)}(\rho)$ is the nominal controller for which its corresponding YK parameter $Q^{(0)}(\rho) = 0$. It is proved that for every continuous/discontinuous interpolating signal γ, $\tilde{K}^{(1)}(\rho,\gamma)$ quadratically stabilizes $G(\rho)$, see[32] for proof. The interpolation method is represented as follows:

- if $\gamma = 0$, $\tilde{K}^{(1)}(\rho,\gamma) \equiv K^{(0)}(\rho)$
- if $\gamma = 1$, $\tilde{K}^{(1)}(\rho,\gamma) \equiv K^{(1)}(\rho)$
- else, $\tilde{K}^{(1)}(\rho,\gamma)$ represents the interpolation between both controllers $K^{(0)}(\rho)$ and $K^{(1)}(\rho)$ according to the chosen γ.

3 Problem Statement

This section defines the considered LPV system with its stabilizing controllers. In addition, it presents the extended parameter region caused by the additional interpolating signal.

3.1 LPV Plant and Controllers Description

Consider a Multi-Input-Multi-Output (MIMO) LPV system $G(\rho)$ with m inputs and p outputs:

$$G(\rho)\begin{cases}\dot{x}(t) = A(\rho(t))x(t) + B_1(\rho(t))w(t) + B_2(\rho(t))u(t) \\ z(t) = C_1(\rho(t))x(t) + D_{11}(\rho(t))w(t) + D_{12}(\rho(t))u(t) \\ y(t) = C_2(\rho(t))x(t) + D_{21}(\rho(t))w(t) + D_{22}(\rho(t))u(t)\end{cases} \tag{6}$$

where $x(t) \in \mathbb{R}^{n_x}$, $y(t) \in \mathbb{R}^p$, $u(t) \in \mathbb{R}^m$, $z(t) \in \mathbb{R}^{n_z}$ are the state, output, input, controlled output vectors respectively. $w(t) = \begin{bmatrix} r & n & d \end{bmatrix}^T \in \mathbb{R}^{n_w}$ contains the exogenous inputs of the tracking reference r, noise n and input disturbance d. $\rho(t) := \rho \in \mathbb{R}^{n_\rho}$ is a vector of n_ρ measurable time-varying parameters.

An LPV system can be handled for control design purpose using different approaches[6]. The polytopic approach is chosen in this work, which requires two assumptions: 1) the system must be strictly proper ($D_{22}(\rho) = 0$); and 2) the input and output matrices B_2, C_2, D_{12} and D_{21} must be parameter-independent[33]. From now on, we assume, without loss of generality, that the LPV system is given as:

$$G(\rho)\begin{cases}\dot{x}(t) = A(\rho)x(t) + B_1(\rho)w(t) + B_2u(t) \\ z(t) = C_1(\rho)x(t) + D_{11}(\rho)w(t) + D_{12}u(t) \\ y(t) = C_2x(t) + D_{21}w(t)\end{cases} \tag{7}$$

Notice that the second assumption does not impose any serious constraints since, if needed, it can be fulfilled by filtering the input u and output y (details are given in[8]). Here, ρ belongs to a convex polytopic region $\mathcal{P}$ defined by the parameters extremums $[\underline{\rho}, \overline{\rho}]$ as:

$$\mathcal{P} := \mathcal{C}_{\mathcal{O}}\{w_1, ..., w_{2^{n_\rho}}\} \tag{8}$$

where w_i represent the vertices of $\mathcal{P}$ $\forall i \in \mathbb{I}[1, 2^{n_\rho}]$. ρ is then scheduled as:

$$\rho = \sum_{i=1}^{2^{n_\rho}} \alpha_i w_i, \tag{9}$$

where $\sum_{i=1}^{2^{n_\rho}} \alpha_i = 1$, $\alpha_i \geq 0$ $\forall i$. Therefore, the system representation at any operating point $\rho \in \mathcal{P}$ is given as a convex combination of the state-space realizations of the LTI systems given at the vertices w_i:

$$\left[\begin{array}{c|cc} A(\rho) & B_1(\rho) & B_2 \\ \hline C_1(\rho) & D_{11}(\rho) & D_{12} \\ C_2 & D_{21} & 0 \end{array}\right] = \sum_{i=1}^{2^{n_\rho}} \alpha_i(\rho) \left[\begin{array}{c|cc} A_i & B_{1,i} & B_2 \\ \hline C_{1,i} & D_{11,i} & D_{12} \\ C_2 & D_{21} & 0 \end{array}\right] \tag{10}$$

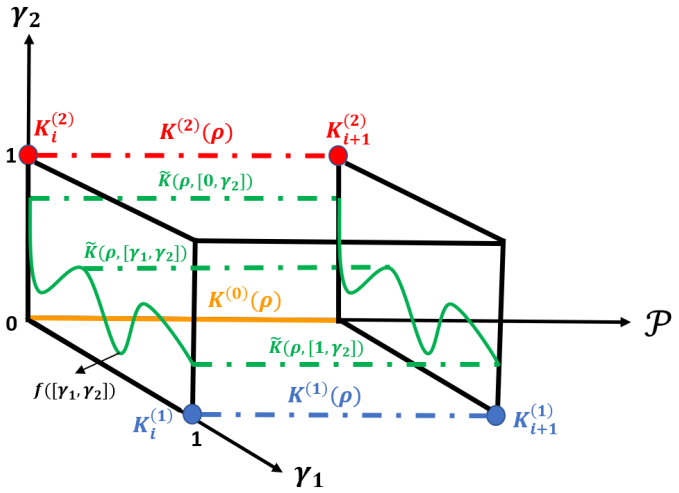

FIGURE 1 Interpolation between three LPV controllers; two YK-based gain-scheduled controllers $K^{(1)}(\rho)$ and $K^{(2)}(\rho)$, and a polytopic-based LPV controller $K^{(0)}(\rho)$ along the convex parameter space $\mathcal{P}$. The LPV-YK controller $\tilde{K}(\rho,\gamma)$ interpolates, using $\gamma=[\gamma_1,\gamma_2]$, between $K^{(0)}(\rho)$ (for $\gamma=[0,0]$), $K^{(1)}(\rho)$ (for $\gamma=[1,0]$), and $K^{(2)}(\rho)$ (for $\gamma=[0,1]$)

Now, assume that

Assumption 1. There exists an LPV output-feedback controller $K^{(0)}(\rho)$ which quadratically stabilizes $G(\rho)$ over $\mathcal{P}$ (following the approach in[8]), defined as:

$$K^{(0)}(\rho):\left[\begin{array}{c|c}A_k^{(0)}(\rho) & B_k^{(0)}(\rho)\\ \hline C_k^{(0)}(\rho) & D_k^{(0)}(\rho)\end{array}\right] \tag{11}$$

being,

$$\left[\begin{array}{c|c}A_k^{(0)}(\rho) & B_k^{(0)}(\rho)\\ \hline C_k^{(0)}(\rho) & D_k^{(0)}(\rho)\end{array}\right]=\sum_{i=1}^{2^{n_p}}\alpha_i(\rho)\left[\begin{array}{c|c}A_{k,i}^{(0)} & B_{k,i}^{(0)}\\ \hline C_{k,i}^{(0)} & D_{k,i}^{(0)}\end{array}\right] \tag{12}$$

where $A_k^{(0)}(\rho)\in\mathbb{R}^{n_k^{(0)}\times n_k^{(0)}}$, $B_k^{(0)}(\rho)\in\mathbb{R}^{n_k^{(0)}\times m_k}$, $C_k^{(0)}(\rho)\in\mathbb{R}^{p_k\times n_k^{(0)}}$ and $D_k^{(0)}(\rho)\in\mathbb{R}^{p_k\times m_k}$.

Assumption 2. At each vertex w_i ($i\in\mathbb{I}[1,2^{n_p}]$) of the polytope $\mathcal{P}$, a group of ζ local LTI controllers $K_i^{(j)}$ ($j\in\mathbb{I}[1,\zeta]$) have been designed separately to stabilize G_i achieving different objectives and performances for all operating conditions.

3.2 Problem Definition

The objective of this work is to:

1. Design a set of gain-scheduled controllers $K^{(j)}(\rho)$, $j\in\mathbb{I}[1,\zeta]$. Each one is designed by interpolating its corresponding LTI controllers $K_i^{(j)}$ ($i\in\mathbb{I}[1,2^{n_p}]$) based on the proposed approach in[14].

2. Create an overall interpolation scheme between the gain-scheduled controllers $K^{(j)}(\rho)$ ($j\in\mathbb{I}[0,\zeta]$), by an interpolating signal vector γ, which is referred to as $\tilde{K}(\rho,\gamma)$, such that the resultant LPV-YK controller $\tilde{K}(\rho,\gamma)$ quadratically stabilizes $G(\rho)$ $\forall\rho\in\mathcal{P}$ and for every $\gamma=[\gamma_1,...,\gamma_j,...,\gamma_\zeta]$.

Figure 1 represents an example of an LPV-YK based interpolation between three gain scheduled-scheduled controllers $K^{(0)}(\rho)$, $K^{(1)}(\rho)$, and $K^{(2)}(\rho)$, along the convex parameter space $\mathcal{P}$. The orange solid line represents the chosen nominal LPV controller $K^{(0)}(\rho)$, as defined by **Assumption 1**. The blue/red points represent the local LTI controllers $K_i^{(1)}/K_i^{(2)}$ ($i\in\mathbb{I}[1,2^{n_p}]$) as defined in **Assumption 2**. The blue/red dashed line is the gain-scheduled controller $K^{(1)}(\rho)/K^{(2)}(\rho)$ that is designed by the YK-based interpolation of the LTI controllers $K_i^{(j)}/K_i^{(2)}$. The overall interpolation is performed using the interpolating signal $\gamma=[\gamma_1,\gamma_2]$, and is represented by the LPV-YK controller $\tilde{K}(\rho,\gamma)$. These LPV and LPV-YK controllers are designed in the next section.

4 Main Results

Based on the statements of LPV concepts and YK parameterization, the LPV-YK controller $\tilde{K}(\rho,\gamma)$ is designed based on a Linear Matrix Inequality (LMI) optimization problem, where it is defined as

$$\tilde{K}(\rho,\gamma) : \left[\begin{array}{c|c} \tilde{A}_k(\rho,\gamma) & \tilde{B}_k(\rho,\gamma) \\ \hline \tilde{C}_k(\rho,\gamma) & \tilde{D}_k(\rho,\gamma) \end{array}\right] \tag{13}$$

It is worth mentioning that for every $\rho \in \mathcal{P}$ and for every continuous/discontinuous interpolating signal γ, $\tilde{K}(\rho,\gamma)$ quadratically stabilizes $G(\rho)$. Some interpolation cases can be mentioned to show how $\tilde{K}(\rho,\gamma)$ recovers a single gain-scheduled controller $K^{(j)}(\rho)$ by varying γ_j:

- if $\gamma_j = 0\ \forall j$, $\tilde{K}(\rho,\gamma) \equiv K^{(0)}(\rho) = \sum_{i=1}^{2^{n_p}} \alpha_i(\rho) K_i^{(0)}$
- if $\gamma_j = 1$ for $j = c \in [1,\zeta]$ and $\gamma_j = 0\ \forall j \neq c$, $\tilde{K}(\rho,\gamma) \equiv K^{(c)}(\rho) = \sum_{i=1}^{2^{n_p}} \alpha_i(\rho) K_i^{(c)}$
- else, the performance of $\tilde{K}(\rho,\gamma)$ is interpolated among $K^{(j)}(\rho)$ according to the chosen γ_j.

Theorem 1. Consider an LPV plant $G(\rho)$ (7), satisfying assumptions **Assumption 1** and **Assumption 2**. Then, the following generalized LPV-YK controller $\tilde{K}(\rho,\gamma)$ (16) quadratically stabilizes $G(\rho)$ for any $\rho \in \mathcal{P}$ and for any continuous/discontinuous interpolating signals $\gamma_j \in [0,1]$ ($j \geq 1$), if there exist symmetric, positive definite, constant matrices $X_g \in \mathbb{R}^{n_x \times n_x}$, $X_{k,i} \in \mathbb{R}^{n_k^{(0)} \times n_k^{(0)}}$, and matrices $W_i \in \mathbb{R}^{m \times n_x}$ and $V_i \in \mathbb{R}^{m \times n_k^{(0)}}$ such that $\forall i$:

$$A_i X_g + X_g A_i^T + B_2 W_i + W_i^T B_2^T < 0 \qquad \forall w_i \tag{14}$$

$$A_{k,i}^{(0)} X_{k,i} + X_{k,i} A_{k,i}^{(0)T} + B_{k,i}^{(0)} V_i + V_i^T B_{k,i}^{(0)T} < 0 \qquad \forall w_i \tag{15}$$

The state-space matrices of $\tilde{K}(\rho,\gamma)$ are

$$\begin{aligned}
\tilde{A}_k(\rho,\gamma) &= \sum_{i=1}^{2^{n_p}} \alpha_i(\rho) \begin{bmatrix} A_i + B_2 F_{g,i} - B_2 \tilde{D}_{q,i}(\gamma) C_2 & -B_2 \tilde{D}_{q,i}(\gamma) F_{k,i}^{(0)} & B_2 \tilde{C}_{q,i}(\gamma) \\ -B_{k,i}^{(0)} C_2 & A_{k,i}^{(0)} & 0 \\ -\tilde{B}_{q,i} C_2 & -\tilde{B}_{q,i} F_{k,i}^{(0)} & \tilde{A}_{q,i} \end{bmatrix} \\
\tilde{B}_k(\rho,\gamma) &= \sum_{i=1}^{2^{n_p}} \alpha_i(\rho) \begin{bmatrix} B_2 \tilde{D}_{q,i}(\gamma) \\ B_{k,i}^{(0)} \\ \tilde{B}_{q,i} \end{bmatrix} \\
\tilde{C}_k(\rho,\gamma) &= \sum_{i=1}^{2^{n_p}} \alpha_i(\rho) \begin{bmatrix} F_{g,i} - (D_{k,i}^{(0)} + \tilde{D}_{q,i}(\gamma)) C_2 & C_{k,i}^{(0)} - \tilde{D}_{q,i}(\gamma) F_{k,i}^{(0)} & \tilde{C}_{q,i}(\gamma) \end{bmatrix} \\
\tilde{D}_k(\rho,\gamma) &= \sum_{i=1}^{2^{n_p}} \alpha_i(\rho) [D_{k,i}^{(0)} + \tilde{D}_{q,i}(\gamma)]
\end{aligned} \tag{16}$$

where $\forall i \in \mathbb{I}[1, 2^{n_p}]$,

$$\begin{aligned}
\tilde{A}_{q,i} &= diag(Z_i^{(1)} A_{q,i}^{(1)} (Z_i^{(1)})^{-1}, \ldots, Z_i^{(j)} A_{q,i}^{(j)} (Z_i^{(j)})^{-1}, \ldots, Z_i^{(\zeta)} A_{q,i}^{(\zeta)} (Z_i^{(\zeta)})^{-1}), \\
\tilde{B}_{q,i} &= \begin{bmatrix} Z_i^{(1)} B_{q,i}^{(1)} & \ldots & Z_i^{(j)} B_{q,i}^{(j)} & \ldots & Z_i^{(\zeta)} B_{q,i}^{(\zeta)} \end{bmatrix}^T, \\
\tilde{C}_{q,i}(\gamma) &= \begin{bmatrix} \gamma_1 C_{q,i}^{(1)} (Z_i^{(1)})^{-1} & \ldots & \gamma_j C_{q,i}^{(j)} (Z_i^{(j)})^{-1} & \ldots & \gamma_\zeta C_{q,i}^{(\zeta)} (Z_i^{(\zeta)})^{-1} \end{bmatrix}, \\
\tilde{D}_{q,i}(\gamma) &= \sum_{j=1}^{\zeta} \gamma_j D_{q,i}^{(j)},
\end{aligned} \tag{17}$$

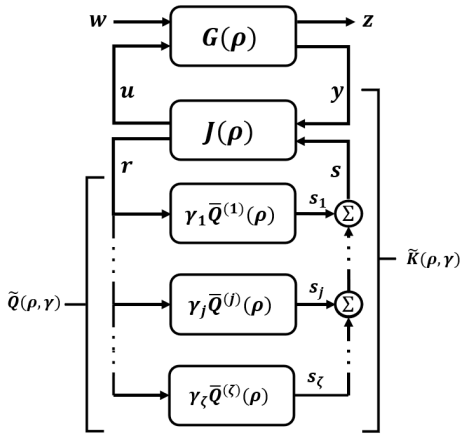

FIGURE 2 LPV-YK LFT configuration

$$Q^{(j)}(\rho)=\sum_{i=1}^{2^{n_p}}\alpha_i(\rho)\left[\begin{array}{c|c}A_{q,i}^{(j)} & B_{q,i}^{(j)}\\ \hline C_{q,i}^{(j)} & D_{q,i}^{(j)}\end{array}\right]=\sum_{i=1}^{2^{n_p}}\alpha_i(\rho)\left[\begin{array}{cc:c|c}A_i+B_2D_{k,i}^{(j)}C_2 & B_2C_{k,i}^{(j)} & B_2[D_{k,i}^{(j)}-D_{k,i}^{(0)}]F_{k,i}^{(0)}-B_2C_{k,i}^{(0)} & B_2[D_{k,i}^{(j)}-D_{k,i}^{(0)}]\\ B_{k,i}^{(j)}C_2 & A_{k,i}^{(j)} & B_{k,i}^{(j)}F_{k,i}^{(0)} & B_{k,i}^{(j)}\\ \hdashline 0 & 0 & A_{k,i}^{(0)}+B_{k,i}^{(0)}F_{k,i}^{(0)} & B_{k,i}^{(0)}\\ \hline [D_{k,i}^{(j)}C_2-F_{g,i}] & C_{k,i}^{(j)} & [(D_{k,i}^{(j)}-D_{k,i}^{(0)})F_{k,i}^{(0)}-C_{k,i}^{(0)}] & [D_{k,i}^{(j)}-D_{k,i}^{(0)}]\end{array}\right] \tag{19}$$

$A_{q,i}^{(j)}$, $B_{q,i}^{(j)}$, $C_{q,i}^{(j)}$ and $D_{q,i}^{(j)}$ are the state-space matrices of $Q^{(j)}(\rho)$ given in (19) at the polytopic vertices w_i, $F_{g,i}=W_iX_g^{-1}$, $F_{k,i}^{(0)}=V_iX_{k,i}^{-1}$, and $Z_i^{(j)}$ are state transformation matrices chosen to satisfy **Lemma 1** such that $\bar{A}_q^{(j)}(\rho)=\sum_{i=1}^{2^{n_p}}\alpha_i(\rho)Z_i^{(j)}A_{q,i}^{(j)}(Z_i^{(j)})^{-1}$ is quadratically stable $\forall j\geq 1$.

Proof 1. According to YK parameterization concept, each parameterized controller can be formulated as a Linear Fractional Transformation (LFT) system, refer to chapter 2 in[21]. Then, the LPV-YK controller can be written as $\tilde{K}(\rho,\gamma)=\mathcal{F}_l(J(\rho),\tilde{Q}(\rho,\gamma))$ (see Fig. 2), where $J(\rho)$ is represented in (18), and $\tilde{Q}(\rho,\gamma)=\sum_{i=1}^{\zeta}\gamma_j(t)\bar{Q}^{(j)}(\rho)$ being $\bar{Q}^{(j)}(\rho)$ a transformed system of $Q^{(j)}(\rho)$ (19) satisfying **Lemma 1**, to be shown later in the proof.

$$J(\rho)=\sum_{i=1}^{2^{n_p}}\alpha_i(\rho)\left[\begin{array}{cc|cc}A_i+B_2F_{g,i} & 0 & 0 & B_2\\ -B_{k,i}^{(0)}C_2 & A_{k,i}^{(0)} & B_{k,i}^{(0)} & 0\\ \hline F_{g,i}-D_{k,i}^{(0)}C_2 & C_{k,i}^{(0)} & D_{k,i}^{(0)} & I\\ -C_2 & -F_{k,i}^{(0)} & I & 0\end{array}\right] \tag{18}$$

The following proof is achieved by two steps: 1) Prove that the LPV-YK parameter $\tilde{Q}(\rho,\gamma)$ is quadratically stable $\forall\rho\in\mathcal{P}$, $\forall\gamma$; and 2) Prove the closed-loop quadratic stability $\forall\rho\in\mathcal{P}$, $\forall\gamma$.

4.1 Step 1:

$\tilde{Q}(\rho,\gamma)$ can be proved to be quadratically stable $\forall\rho\in\mathcal{P}$ and $\forall\gamma$ as follows:
Assuming **Assumption 2**, and since inequality (15) is satisfied, there exist symmetric, positive definite matrices $S_i^{(j)}\in\mathbb{R}^{(n_x+n_k^{(j)})\times(n_x+n_k^{(j)})}$ and $R_i\in\mathbb{R}^{n_k^{(0)}\times n_k^{(0)}}$ such that $\forall i,\forall j\geq 1$:

$$S_i^{(j)}\mathcal{A}_i^{(j)}+\mathcal{A}_i^{(j)T}S_i^{(j)}<0 \tag{20}$$

$$(A_{k,i}^{(0)}+B_{k,i}^{(0)}F_{k,i}^{(0)})R_i+R_i(A_{k,i}^{(0)}+B_{k,i}^{(0)}F_{k,i}^{(0)})^T<0 \tag{21}$$

$$CL(\rho,\gamma)=\sum_{i=1}^{2^{n_p}}\alpha_i(\rho)\left[\begin{array}{ccc|c} A_i+B_2(D_{k,i}^{(0)}+\tilde{D}_{q,i}(\gamma))C_2 & B_2(F_{g,i}-(D_{k,i}^{(0)}+\tilde{D}_{q,i}(\gamma))C_2) & B_2(C_{k,i}^{(0)}-\tilde{D}_{q,i}(\gamma)F_{k,i}^{(0)}) & B_2\tilde{C}_{q,i}(\gamma) & B_{1,i}+B_2(D_{k,i}^{(0)}+\tilde{D}_{q,i}(\gamma))D_{21}\\ B_2\tilde{D}_{q,i}(\gamma)C_2 & A_i+B_2(F_{g,i}-\tilde{D}_{q,i}(\gamma)C_2) & -B_2\tilde{D}_{q,i}(\gamma)F_{k,i}^{(0)} & B_2\tilde{C}_{q,i}(\gamma) & B_2\tilde{D}_{q,i}(\gamma)D_{21}\\ B_{k,i}^{(0)}C_2 & -B_{k,i}^{(0)}C_2 & A_{k,i}^{(0)} & 0 & B_{k,i}^{(0)}D_{21}\\ \tilde{B}_{q,i}C_2 & -\tilde{B}_{q,i}C_2 & -\tilde{B}_{q,i}F_{k,i}^{(0)} & \tilde{A}_{q,i} & \tilde{B}_{q,i}D_{21}\\ \hline C_{1,i}+D_{12}(D_{k,i}^{(0)}+\tilde{D}_{q,i}(\gamma))C_2 & D_{12}(F_{g,i}-(D_{k,i}^{(0)}+\tilde{D}_{q,i}(\gamma))C_2) & D_{12}(C_{k,i}^{(0)}-\tilde{D}_{q,i}(\gamma)F_{k,i}^{(0)}) & D_{12}\tilde{C}_{q,i}(\gamma) & D_{11,i}+D_{12}(D_{k,i}^{(0)}+\tilde{D}_{q,i}(\gamma))D_{21} \end{array}\right] \tag{24}$$

$$\bar{A}_{cl}(\rho,\gamma)=\sum_{i=1}^{2^{n_p}}\alpha_i(\rho)TA_{cl,i}(\gamma)T^{-1}=\sum_{i=1}^{2^{n_p}}\alpha_i(\rho)\left[\begin{array}{cc:cc} A_i+B_2F_{g,i} & B_2\tilde{C}_{q,i}(\gamma) & -B_2(F_{g,i}-(D_{k,i}^{(0)}+\tilde{D}_{q,i}(\gamma))C_2) & B_2(C_{k,i}^{(0)}-\tilde{D}_{q,i}(\gamma)F_{k,i}^{(0)})\\ 0 & \tilde{A}_{q,i} & \tilde{B}_{q,i}C_2 & -\tilde{B}_{q,i}F_{k,i}^{(0)}\\ \hdashline 0 & 0 & A_i+B_2D_{k,i}^{(0)}C_2 & B_2C_{k,i}^{(0)}\\ 0 & 0 & B_{k,i}^{(0)}C_2 & A_{k,i}^{(0)} \end{array}\right] \tag{26}$$

being,

$$\mathcal{A}_i^{(j)}=\left[\begin{array}{cc} A_i+B_2D_{k,i}^{(j)}C_2 & B_2C_{k,i}^{(j)}\\ B_{k,i}^{(j)}C_2 & A_{k,i}^{(j)} \end{array}\right] \tag{22}$$

with $R_i = X_{k,i}$ and $F_{k,i}^{(0)} = V_iX_{k,i}^{-1}$. Thus, $A_{q,i}^{(j)}$ is Hurwitz $\forall i,j$ and there exist symmetric, positive definite matrices $X_{q,i}^{(j)} = diag(S_i^{(j)}, R_i) \in \mathbb{R}^{n_{q,i}^{(j)}\times n_{q,i}^{(j)}}$ such that:

$$X_{q,i}^{(j)}A_{q,i}^{(j)}+(A_{q,i}^{(j)})^TX_{q,i}^{(j)}<0 \qquad \forall i,\forall j \tag{23}$$

Following **Lemma 1**, for any $j \geq 1$, there exist transformation matrices $Z_i^{(j)}$ such that the transformed system $\bar{Q}^{(j)}(\rho)$ is quadratically stable $\forall\rho \in \mathcal{P}^{(j)}$, choose $Z_i^{(j)} = (X_{q,i}^{(j)})^{1/2}$. As a result, $\tilde{Q}(\rho,\gamma) = \sum_{j=1}^{\zeta}\gamma_j\bar{Q}^{(j)}(\rho)$ is quadratically stable $\forall\rho \in \mathcal{P}$ and $\forall\gamma \in [0,1]$.

4.2 Step 2:

The closed-loop system $CL(\rho,\gamma)$ (24) is derived from the LFT interconnection between $G(\rho)$ and $\tilde{K}(\rho,\gamma)$ (see Fig. 3). The closed-loop state matrix $A_{cl}(\rho,\gamma) = \sum_{i=1}^{2^{n_p}}\alpha_i(\rho)A_{cl,i}(\gamma)$ is quadratically stable if there exist a symmetric, positive definite, constant matrix X_{cl} such that:

$$X_{cl}A_{cl}(\rho,\gamma)+A_{cl}^T(\rho,\gamma)X_{cl}<0 \qquad \forall\gamma \tag{25}$$

Now , let $T=\begin{bmatrix} I & 0 & 0 & 0\\ 0 & 0 & 0 & I\\ I & -I & 0 & 0\\ 0 & 0 & I & 0 \end{bmatrix}$ be a state transformation matrix which is applied to $CL(\rho,\gamma)$ without changing its input-output nature, with $T^{-1}=\begin{bmatrix} I & 0 & 0 & 0\\ I & 0 & -I & 0\\ 0 & 0 & 0 & I\\ 0 & I & 0 & 0 \end{bmatrix}$.

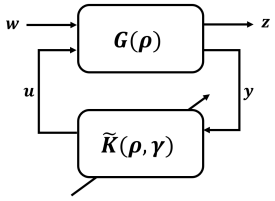

FIGURE 3 $G - \tilde{K}$ LFT interconnection

Due to the block-triangular form of $\bar{A}_{cl}(\rho,\gamma)$ (26) , (25) is satisfied if the following equations hold (check *Lemma 2* in [18]):

$$\sum_{i=1}^{2^{n_p}} \alpha_i(\rho)(Y_g(A_i + B_2F_{g,i}) + (A_i + B_2F_{g,i})^T Y_g) < 0 \tag{27}$$

$$\sum_{i=1}^{2^{n_p}} \alpha_i(\rho)(Y_q\tilde{A}_{q,i} + \tilde{A}_{q,i}^T Y_q) < 0 \tag{28}$$

$$\sum_{i=1}^{2^{n_p}} \alpha_i(\rho)(Y_0\mathcal{A}_i^{(0)} + \mathcal{A}_i^{(0)T} Y_0) < 0 \tag{29}$$

where $Y_g \in \mathbb{R}^{n_x\times n_x}$, $Y_q \in \mathbb{R}^{n_q^{(1)}\times n_q^{(1)}}$ and $Y_0 \in \mathbb{R}^{(n_x+n_k^{(0)})\times(n_x+n_k^{(0)})}$ are symmetric, positive definite, parameter-invariant matrices, with $X_{cl} = T^T \operatorname{diag}(Y_g, Y_q, Y_0)\, T$, and

$$\mathcal{A}_i^{(0)} = \begin{bmatrix} A_i + B_2D_{k,i}^{(0)}C_2 & B_2C_{k,i}^{(0)} \\ B_{k,i}^{(0)}C_2 & A_{k,i}^{(0)} \end{bmatrix} \tag{30}$$

- Inequality (27) is equivalent to (14) by choosing $Y_g = X_g^{-1}$ and $W_i = F_{g,i}X_g$.
- Since $\tilde{Q}(\rho,\gamma)$ is proved to be quadratically stable, inequality (28) is satisfied.
- (29) is fulfilled given that $K^{(0)}(\rho)$ quadratically stabilizes $G(\rho)$.

It is worth mentioning that the problem complexity refers mainly to find a nominal LPV controller $K^{(0)}(\rho)$ which must quadratically stabilize $G(\rho)$, i.e. assumption **Assumption 1**. The rest is carried out using classical LTI control approaches. This shows an interest since a quadratically stabilizing gain-scheduled controller $K^{(j)}(\rho)$ could be designed based on an interpolation of LTI controllers, with lower conservatism compared to the standard polytopic design [8]. In addition, the interpolation of several gain-scheduled controllers, with any finite continuous/discontinuous interpolating signals γ_j, provides a general multi-variable and multi-objective controller $\tilde{K}(\rho,\gamma)$ based on LPV-YK concept.

5 LPV-YK Control Implementation

In this section, the implementation scheme of the LPV-YK control is formulated using the doubly coprime factorization [31].

5.1 Coprime Factorization

Using the doubly coprime factorization concept, at each vertex w_i of $\mathcal{P}$, the plant model G_i and the controllers $K_i^{(j)}, \forall i \in \mathbb{I}[1, 2^{n_p}]$ and $\forall j \in \mathbb{I}[0, \zeta]$, can be factorised as:

$$\begin{aligned} G_i &= N_iM_i^{-1} = \tilde{M}_i^{-1}\tilde{N}_i \\ K_i^{(j)} &= U_i^{(j)}V_i^{(j)-1} = \tilde{V}_i^{(j)-1}\tilde{U}_i^{(j)} \end{aligned} \tag{31}$$

Lemma 2 is applied $\forall i, \forall j$, where the coprime factors are computed such that M_i, N_i, $\tilde{M}_i$, $\tilde{N}_i$, $U_i^{(j)}$, $V_i^{(j)}$, $\tilde{U}_i^{(j)}$, $\tilde{V}_i^{(j)} \in \mathcal{RH}_\infty$ and satisfying the following *Bezout Identity*:

$$\begin{bmatrix} \tilde{V}_i^{(j)} & -\tilde{U}_i^{(j)} \\ -\tilde{N}_i & \tilde{M}_i \end{bmatrix} \begin{bmatrix} M_i & U_i^{(j)} \\ N_i & V_i^{(j)} \end{bmatrix} = \begin{bmatrix} M_i & U_i^{(j)} \\ N_i & V_i^{(j)} \end{bmatrix} \begin{bmatrix} \tilde{V}_i^{(j)} & -\tilde{U}_i^{(j)} \\ -\tilde{N}_i & \tilde{M}_i \end{bmatrix} = \begin{bmatrix} I & 0 \\ 0 & I \end{bmatrix} \tag{32}$$

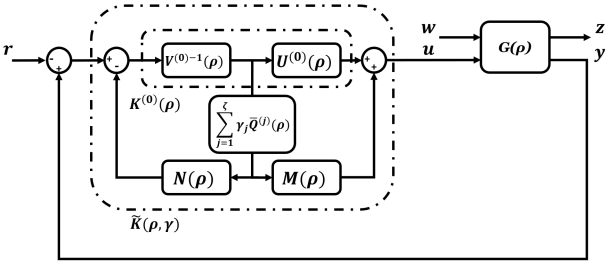

FIGURE 4 YK control structure

The coprime factors are computed at each vertex using the state-space representations written in (33)-(34).

$$\begin{bmatrix} M_i & U_i^{(j)} \\ N_i & V_i^{(j)} \end{bmatrix} : \left[\begin{array}{cc|cc} A_i + B_2F_{g,i} & 0 & B_2 & 0 \\ 0 & A_{k,i}^{(j)} + B_{k,i}^{(j)}F_{k,i}^{(j)} & 0 & B_{k,i}^{(j)} \\ \hline F_{g,i} & C_{k,i}^{(j)} + D_{k,i}^{(j)}F_{k,i}^{(j)} & I & D_{k,i}^{(j)} \\ C_2 & F_{k,i}^{(j)} & 0 & I \end{array}\right] \tag{33}$$

$$\begin{bmatrix} \tilde{V}_i^{(j)} & -\tilde{U}_i^{(j)} \\ -\tilde{N}_i & \tilde{M}_i \end{bmatrix} : \left[\begin{array}{cc|cc} A_i + B_2D_{k,i}^{(j)}C_2 & B_2C_{k,i}^{(j)} & -B_2 & B_2D_{k,i}^{(j)} \\ B_{k,i}^{(j)}C_2 & A_{k,i}^{(j)} & 0 & B_{k,i}^{(j)} \\ \hline F_{g,i} - D_{k,i}^{(j)}C_2 & -C_{k,i}^{(j)} & I & -D_{k,i}^{(j)} \\ C_2 & -F_{k,i}^{(j)} & 0 & I \end{array}\right] \tag{34}$$

5.2 LPV-YK Control Structure

Recall that $K^{(0)}(\rho)$ is previously designed to quadratically stabilize $G(\rho)$ (7), and the gain-scheduled controllers $K^{(j)}(\rho)$ are designed using **Theorem 1** to quadratically stabilize $G(\rho)$. Following **Lemma 3**, and choosing $K^{(0)}(\rho)$ as the nominal controller, the generalized LPV-YK controller $\tilde{K}(\rho,\gamma)$ can be expressed as:

$$\begin{aligned} \tilde{K}(\rho,\gamma) &= \Big(U^{(0)}(\rho) + M(\rho)\sum_{j=1}^{\zeta}\gamma_j\bar{Q}^{(j)}(\rho)\Big)\Big(V^{(0)}(\rho) + N(\rho)\sum_{j=1}^{\zeta}\gamma_j\bar{Q}^{(j)}(\rho)\Big)^{-1} \\ &= \Big(\tilde{V}^{(0)}(\rho) + \sum_{j=1}^{\zeta}\gamma_j\bar{Q}^{(j)}(\rho)\tilde{N}(\rho)\Big)^{-1}\Big(\tilde{U}^{(0)}(\rho) + \sum_{j=1}^{\zeta}\gamma_j\bar{Q}^{(j)}(\rho)\tilde{M}(\rho)\Big) \end{aligned} \tag{35}$$

5.3 How to choose the interpolating signal vector γ

γ is a vector of interpolating signals γ_j, where each one multiplies its corresponding output of $\bar{Q}^{(j)}(\rho)$ to interpolate between several parameterized controllers $K^{(j)}(\rho) = \mathcal{F}_l(J(\rho), \bar{Q}^{(j)}(\rho))$. Notice that γ_j could be any ad-hoc physically based, continuous/discontinuous, external or internal signals. Theoretically, and according to the proof above, the closed-loop quadratic stability is achieved for any γ_j having finite positive/negative value with any rate of variation. However, for control interpolation, the interpolating signals γ_j are chosen to be in $[0, 1]$. In this paper, γ_j are chosen as

$$\sum_{j=1}^{\zeta}\gamma_j = 1, \quad \gamma_j \in [0,1]\ \forall j \tag{36}$$

5.4 Local LTI Control Performance Recovery

In this section, the performance recovery of each pre-designed local LTI controller $K_i^{(j)}$ ($i \in [1, 2^{n_p}]$, $j \geq 1$), from the LPV-YK controller $\tilde{K}(\rho,\gamma)$, is verified. Let us choose an LTI controller $K_l^{(c)}$ (i.e. $\gamma_c = 1$ and $\gamma_j = 0\ \forall j \neq c$, and $\rho = w_l$). The following derivation shows the performance recovery of of $K_l^{(c)}$ from $\tilde{K}(\rho,\gamma)$:

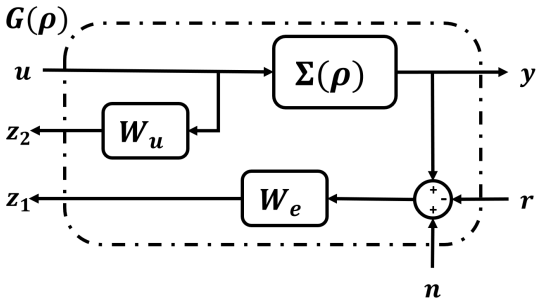

FIGURE 5 Generalized Plant $G(\rho)$

Substitute the vertex $w_l^{(c)}$ and $\gamma = [0 \dots 0 \;\; \gamma_c = 1 \;\; 0 \dots 0]$ (denoted by $\gamma_c^* = 1$) in (35),

$$\tilde{K}(w_l, \gamma_c^* = 1) = \left(U_l^{(0)} + M_l \bar{Q}_l^{(c)}\right)\left(V_l^{(0)} + N_l \bar{Q}_l^{(c)}(\rho)\right)^{-1} \tag{37}$$

Since the input-output performance of Q and $\bar{Q}$ is similar (according to the state transformation concept), $\bar{Q}_l^{(0)} \equiv Q_l^{(0)}$. According to[21], (37) can be written as

$$\tilde{K}(w_l, \gamma_c^* = 1) = U_l^{(0)}(V_l^{(0)})^{-1} + (\tilde{V}_l^{(0)})^{-1} Q_l^{(c)} \left(I + (V_l^{(0)})^{-1} N_l^{(0)} Q_l^{(c)}\right)^{-1} (V_l^{(0)})^{-1} \tag{38}$$

Referring to YK concept, $Q_l^{(c)} = \tilde{U}_l^{(c)} V_l^{(0)} - \tilde{V}_l^{(c)} U_l^{(0)}$, after some derivations:

$$\begin{aligned} Q_l^{(c)} &= \tilde{V}_l^{(c)} (\tilde{V}_l^{(c)})^{-1} \tilde{U}_l^{(c)} V_l^{(0)} - \tilde{V}_l^{(c)} U_l^{(0)} (V_l^{(0)})^{-1} V_l^{(0)} \\ &= \tilde{V}_l^{(c)} K_l^{(c)} V_l^{(0)} - \tilde{V}_l^{(c)} K_l^{(0)} V_l^{(0)} \\ &= \tilde{V}_l^{(c)} (K_l^{(c)} - K_l^{(0)}) V_l^{(0)} \end{aligned} \tag{39}$$

Substitute and shape it, then

$$\tilde{K}(w_l, \gamma_c^* = 1) = K_l^{(0)} + [\tilde{V}_l^{(c)} V_l^{(0)} + (K_l^{(c)} - K_l^{(0)}) N_l \tilde{V}_l^{(0)}]^{-1} \times (K_l^{(c)} - K_l^{(0)}) \tag{40}$$

Knowing that $K_l^{(c)} = (\tilde{V}_l^{(c)})^{-1} \tilde{U}_l^{(c)}$, and applying the Bezout identities (32), we get:

$$\tilde{V}_l^{(c)} V_l^{(0)} + (K_l^{(c)} - K_l^{(0)}) N_l \tilde{V}_l^{(0)} = I. \tag{41}$$

Then,

$$\tilde{K}(w_l, \gamma_c^* = 1) = K_l^{(0)} + K_l^{(c)} - K_l^{(0)} = K_l^{(c)}. \tag{42}$$

Therefore, it is shown that the performance achieved by the LPV-YK controller $\tilde{K}(\rho, \gamma)$ at any vertex w_l is equivalent to the performance of its corresponding LTI controller $K_l^{(c)}$.

6 Application to Autonomous Vehicles

The proposed method is applied here to the autonomous vehicle lateral control.[30] compares three LPV control approaches where the longitudinal speed is considered as the varying parameter. In addition, lateral control aims to achieve various objectives such as lane tracking, lane changing, obstacle avoidance, etc. Consequently, various performances are required accordingly for different traffic situations that faces the vehicle. Thus, an LPV-YK controller could be designed to achieve multiple objectives, depending on the driving situation, over the full vehicle speed range.

6.1 Lateral Bicycle Model

We consider here the well known bicycle model of an autonomous vehicle. The non-linear lateral dynamics can be written as a polytopic LPV model $\Sigma(\rho)$[30]:

$$\Sigma(\rho) \begin{cases} \dot{x}(t) = A_\Sigma(\rho) x(t) + B_\Sigma u(t) \\ y(t) = C_\Sigma x(t) \end{cases} \tag{43}$$

being

$$x(t) = \begin{bmatrix} v_y \\ w \end{bmatrix},\ u(t) = \delta,\ B_\Sigma = \begin{bmatrix} \frac{1}{m}C_f \\ \frac{1}{I}C_f l_f \end{bmatrix},\ C_\Sigma = \begin{bmatrix} 0 & 1 \end{bmatrix}, A_\Sigma(\rho) = \begin{bmatrix} -\frac{C_r+C_f}{m}\rho_2 & -\frac{C_f l_f - C_r l_r}{m}\rho_2 - \rho_1 \\ -\frac{C_f l_f - l_r C_r}{I}\rho_2 & -\frac{C_f l_f^2 + l_r^2 C_r}{I}\rho_2 \end{bmatrix}, \tag{44}$$

where $\rho = [\rho_1, \rho_2] = [v_x, \frac{1}{v_x}]$. v_x represents the longitudinal speed which varies in $[1, 30]$ m/s. v_y and w are the lateral and rotational velocities in the vehicle's frame, respectively. δ is the control input, the steering angle of the front tire. C_f and C_r represent the stiffness of the front and rear wheel-tires. I, m, l_f and l_r are the vehicle's inertia, mass and the distance from the center of gravity to the front and rear wheel axes respectively.

6.2 Lateral Control Design

In this work, the control design problems (mentioned in **Assumption 1**-**Assumption 2**) are solved using the $\mathcal{H}_\infty$ concept. For control design purpose, two weighting transfer functions $W_e(s)$ and $W_u(s)$ are designed to present the tracking performance and the actuator limitations respectively. Then, the state-space representation of $G(\rho)$ is obtained from the generalized plant shown in Fig. 5. $G(\rho)$ is written as a convex combination of the vertices of the polytope $\mathcal{P} = \mathcal{C}_\mathcal{O}\{(\underline{\rho_1}, \underline{\rho_2}), (\underline{\rho_1}, \overline{\rho_2}), (\overline{\rho_1}, \underline{\rho_2}), (\overline{\rho_1}, \overline{\rho_2})\}$ (refer to (9)-(10)).

Now, following **Assumption 1**- **Assumption 2**, a highly robust LPV controller $K^{(0)}(\rho)$, and two gain-scheduled controllers $K^{(1)}(\rho)$ and $K^{(2)}(\rho)$ are designed to perform different required performances as follows:

- The polytopic-based LPV controller $K^{(0)}(\rho)$ is designed using the $\mathcal{H}_\infty$ concept following a method similar to [8]. A slow transient response and noise rejection performances are required for the nominal controller $K^{(0)}(\rho)$ using weighting functions $W_e^{(0)}$ and $W_u^{(0)}$.
- LTI controllers $K_i^{(1)}$ are designed separately using LTI/$\mathcal{H}_\infty$ concept at each vertex w_i to perform smooth lateral transitions which is important to provide comfort riding. This is achieved using certain weighting functions $W_e^{(1)}$ and $W_u^{(1)}$ $\forall i$.
- LTI controllers $K_i^{(2)}$ are designed separately using LTI/$\mathcal{H}_\infty$ concept at each vertex w_i to perform fast lateral transitions to handle the vehicle when facing aggressive maneuvers and lateral oscillations. The chosen weighting functions are $W_e^{(2)}$ and $W_u^{(2)}$ $\forall i$.

6.3 Design the LPV-YK Control Structure

The following steps are done to design the LPV-YK control shown in Fig. 4:

- According to the method explained in Section 4 and **Theorem 1**, the LPV polytopic-based state-feedback controller $F_g(\rho)$, and the LTI state-feedback controllers $F_{k,i}^{(0)}$, $\forall i \in \mathbb{I}[1, 4]$, can be designed using an LMI-based state-feedback approach (pole-placement constraints or Linear Quadratic Regulator).
- The state-space representations of $M(\rho)$, $N(\rho)$, $U^{(0)}(\rho)$ and $V^{(0)}(\rho)$ are computed as illustrated in Section 5.1, and $Q^{(j)}(\rho, \gamma)$ ($j \in \{1, 2\}$) is obtained from (19).

Remark 1. All the LPV systems $V^{(0)-1}(\rho)$, $U^{(0)}(\rho)$, $N(\rho)$, $M(\rho)$, and $Q^{(j)}(\rho)$ $(\forall j)$ are implemented in their state-space representations i.e. each LPV system is self-scheduled according to the change of the varying parameter ρ.
Simultaneously, to switch between LPV controllers, the switching signals γ_j's are used to choose the LPV-YK parameter $Q^{(j)}(\rho)$ that corresponds to the LPV controller $K^{(j)}(\rho)$. For more illustration, to switch from $K^{(1)}(\rho)$ to $K^{(2)}(\rho)$, we assign $\gamma_1 = 0$ and $\gamma_2 = 1$.

Here, the interpolating signal $\gamma(t)$ is a vector of dimension two $[\gamma_1(t), \gamma_2(t)]$, where each γ_j multiplies its corresponding $Q^{(j)}(\rho)$. In this example, and based on an experimental experience, $\gamma_2(t)$ is chosen to vary according to the demanded control tasks. Linear relations are proposed between different variables as follows:

- if $\theta_e \leq 0.1$, $\gamma_2(t) = sat(-y_L + 1.4 + 0.1\dot{\delta}, [0, 1])$
- if $\theta_e > 0.1$, $\gamma_2(t) = sat(-0.7y_e + 1.4, [0, 1])$

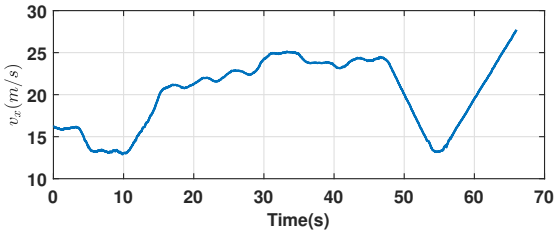

FIGURE 6 Simulation: Parameter-varying longitudinal speed v_x (m/s)

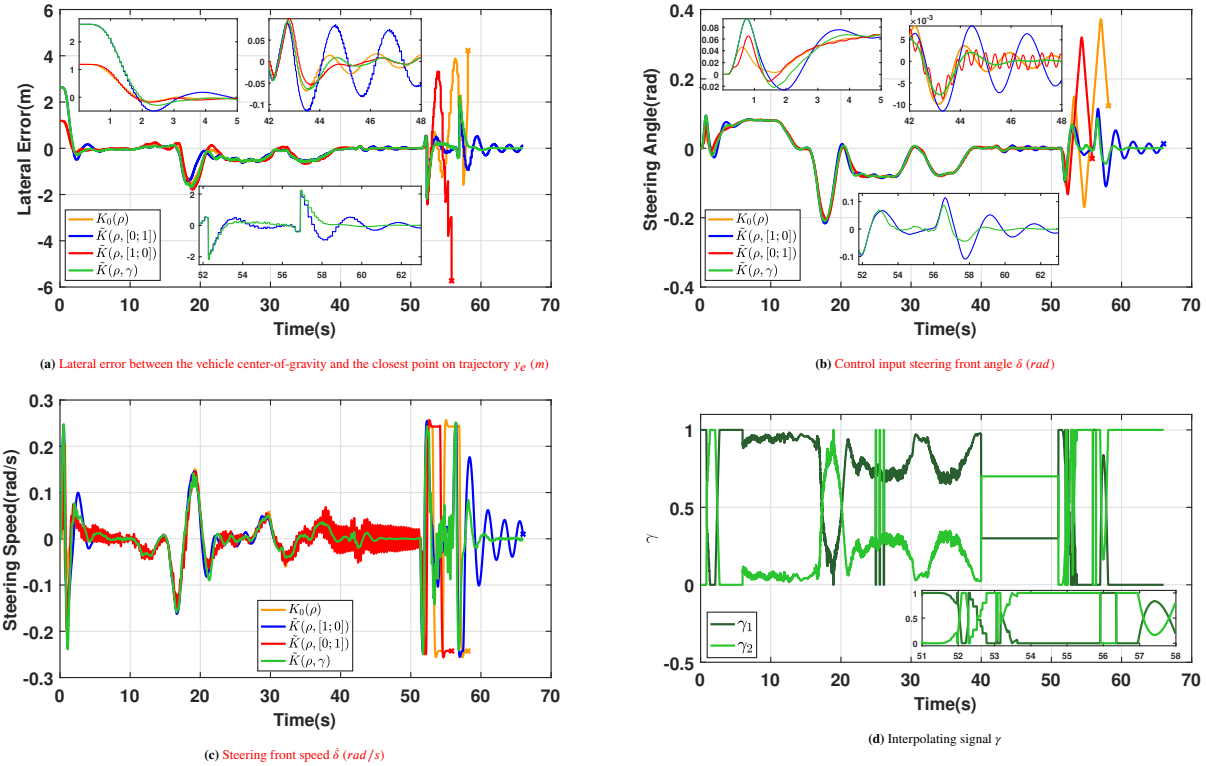

(a) Lateral error between the vehicle center-of-gravity and the closest point on trajectory y_e (m)

(b) Control input steering front angle δ (rad)

(c) Steering front speed $\dot{\delta}$ (rad/s)

(d) Interpolating signal γ

FIGURE 7 Simulation results

- $\gamma_1(t) = 1 - \gamma_2(t)$

where θ_e and y_e represent the heading and lateral errors between the vehicle and the current point on the reference path, respectively. $\dot{\delta}$ is the steering speed, and y_L is the lateral error at a look-ahead distance L[34].

6.4 Simulation Results

The parameterized LPV-YK controller $\tilde{K}(\rho,\gamma)$ is structured as shown in Fig. 4 and simulated on a nonlinear full car model designed for a Renault ZOE vehicle. The simulation is done using a part of a real trajectory map (*Satory*) where its coordinates are obtained from a pre-recorded map using a positioning system mounted on a real vehicle. The real vehicle speed from this recording is multiplied by 1.7 gain and used as a speed profile reference, to test the controllers within critical high speeds).

A scenario is chosen to cover several lateral tasks and critical situations as follows: 1) the vehicle is required to start its Autonomous Driving (AD) with a large lateral error ($y_e > 2\,m$); 2) When $t \in [10, 40]s$, the vehicle performs four successive turns at a high speed ($v_x > 20m/s$); 3) When $t \in [40, 50]s$, the vehicle is subjected to some sensor noises (due to real measurements)

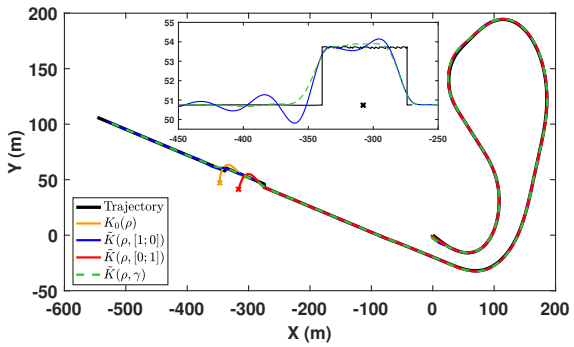

FIGURE 8 Simulation: Planned and controlled trajectories

on a straight stretch; and finally 4) An obstacle is detected when $t \in [50, 60]s$, the navigation modifies the trajectory suddenly as two successive lateral steps (each one of 3 m), aiming to avoid a collision.

The scenario is tested with different controllers: $\tilde{K}(\rho,[0,0]) \equiv K^{(0)}(\rho)$ (the nominal high robust controller), $\tilde{K}(\rho,[1,0]) \equiv K^{(1)}(\rho)$ (smooth tracker), $\tilde{K}(\rho,[0,1]) \equiv K^{(2)}(\rho)$ (aggressive tracker), and our proposed controller $\tilde{K}(\rho,\gamma)$ with $\gamma = [\gamma_1, \gamma_2]$ varies in real-time. Fig. 6 shows the speed profile for all the tests. Fig. 7a depicts the lateral error from the reference trajectory to the vehicle Center of Gravity (CoG), and the steering control input is shown in Fig. 7b. Fig. 7c represents the steering speed which reflects the driving comfort. Fig. 7d shows the evolution of the interpolating signal γ for $\tilde{K}(\rho,\gamma)$, and Fig. 8 shows the (X-Y) coordinates of the reference trajectory and the vehicle positioning response of the different tested controllers. The sub-figures in Figs. 7 and 8 show some zoomed results over time.

At $t = 0s$, it is shown in Fig. 7a that not all the tested controllers are activated to start at high lateral error ($y_e > 2.5m$), since both controllers $K^{(0)}(\rho)$ and $\tilde{K}(\rho,[0,1])$ can't deal with large lateral errors (observed from pre-testing). On the other hand, $\tilde{K}(\rho,[1,0])$ and $\tilde{K}(\rho,\gamma)$ perform better with the initial high lateral error, where $\tilde{K}(\rho,\gamma)$ shows a lower overshoot (see Fig. 7a when $t \in [2,5]s$) with a smoother steering action (see Fig. 7b when $t \in [2,4]s$). During the four successive turns, the four tested controllers have almost similar tracking performance (check Fig. 7a), where there exists low steering noises using the fast controller $\tilde{K}(\rho,[0,1])$ as shown in Fig. 7c.

When $t \in [42,48]s$ (on the straight highway), Fig. 7a shows that the slow controllers ($K^{(0)}(\rho)$, $\tilde{K}(\rho,[1,0])$) have lateral oscillations due to actuator limitations (for smoothness). On the other hand, the fast controller $\tilde{K}(\rho,[0,1])$ could handle the vehicle, but demanding more steering effort with noises (see Fig. 7c when $t \in [42,48]s$). However, due to the use of the steering speed in the proposed equations of γ_2, γ changes to $[0.3, 0.7]$, and $\tilde{K}(\rho,\gamma)$ achieves a perfect trade-off between decreasing the lateral oscillations (in Fig. 7a) and relaxing the steering action (in Fig. 7b and 7c).

Finally, it is clear in Fig. 8 that both $K^{(0)}(\rho)$ and $\tilde{K}(\rho,[0,1])$ could not perform a fast double lane-change to overcome an obstacle (represented as "**x**"). Although the smooth controller $\tilde{K}(\rho,[1,0])$ could succeed in performing it, however, the vehicle performs high lateral oscillations. On the other hand, $\tilde{K}(\rho,\gamma)$ shows better performance without any lateral overshoots (see Fig. 7a when $t \in [52,62]s$) and with a very smooth and optimized steering action (see Fig. 7b and 7c when $t \in [52,62]s$). Thanks to the variations of γ which reflects the needed lateral task to the proposed parameterized controller $\tilde{K}(\rho,\gamma)$, obtaining a combination between the designed performances.

Table 1 summarizes the conclusions behind the simulation results. Each of the controllers $K^{(0)}(\rho)$, $K^{(1)}(\rho)$, and $K^{(2)}(\rho)$ has some advantages and disadvantages. Generally speaking, $K^{(0)}(\rho)$ has shown high robustness, however it deteriorates its tracking accuracy. In addition, $K^{(1)}(\rho)$ achieves good tracking performance, while it is not capable to handle the vehicle at high lateral accelerations. Moreover, $K^{(2)}(\rho)$ is designed to handle high lateral accelerations which make it more sensitive to noises at high frequencies. Therefore, the solution is to use all the controllers, where each one is used in its preferred situation, which is achieved using the proposed LPV-YK controller $\tilde{K}(\rho,\gamma)$. Notice that $\tilde{K}(\rho,\gamma)$ hasn't shown any performance deterioration in all driving situations.

TABLE 1 Overview of the tested controllers in simulation

Controller	Value of interpolating vector γ	Control objective	Advantages	Disadvantages
$\tilde{K}(\rho,[0,0]) \equiv K^{(0)}(\rho)$	[0,0]	Highly robust	High noise rejection due to bad environment conditions, sensor faults, etc.	Inaccurate tracking performance and conservative
$\tilde{K}(\rho,[1,0]) \equiv K^{(1)}(\rho)$	[1,0]	Smooth tracker	Good tracking performance with smooth steering	Oscillatory and cannot perform well at high lateral accelerations
$\tilde{K}(\rho,[0,1]) \equiv K^{(2)}(\rho)$	[0,1]	Aggressive tracker	Fast tracking performance and could achieve high lateral accelerations	Too sensitive to noises
$\tilde{K}(\rho,\gamma)$	variant as in Fig. 7d	Multiple objectives by varying the interpolating vector γ.	All the mentioned advantages and even more by choosing the optimal combination of controllers by γ	No bad performance is observed

FIGURE 9 Renault ZOE automated vehicle

7 Experimental Results

The LPV-YK controller $\tilde{K}(\rho,\gamma)$ is tested on a robotized electric Renault ZOE vehicle shown in Fig. 9. It is prepared for lateral and longitudinal controls by computer-controlled steering and pedal actuators. Vehicle speed and the global coordinates are measurable using GPS and IMU. Previously, we have tested a polytopic-based LPV controller $K_1(\rho)$ which has been designed with the weights $W_e^{(1)}$ and $W_u^{(1)}$ (i.e. the same used to design $\tilde{K}(\rho,[1,0])$), and using the standard polytopic optimisation problem[4]. Notice that the interpolating signal vector γ is switched manually during the test. This section aims mainly to: 1) Compare both controllers $K_1(\rho)$ and $\tilde{K}(\rho,[1,0])$; and 2) Observe the controller response when switching γ rapidly as a step.

The test is done in a part of *Satory* test-track shown in Fig. 10. This test-track is challenging concerning the bad road conditions and its inclinations. Fig. 11a shows the variation of the measured longitudinal speed in Kph which is considered to be coherent with respect to the road curvature. The vehicle starts on a straight highway using the smooth controller $\tilde{K}(\rho,[1,0])$. Then, it switches to the faster controller $\tilde{K}(\rho,[0,1])$ when approaching two successive maneuvers (at $t = 20s$) aiming to achieve the lowest lateral error. After exiting the successive maneuvers, it switches again to the smooth controller $\tilde{K}(\rho,[1,0])$ (at $t = 50s$) and enters a second maneuver to compare its performance to the previously tested polytopic LPV controller $K_1(\rho)$.

Regarding Figs. 11c and 11d, it is clearly shown that the vehicle performance is not affected during the switching times (at $t = 20s$ and $t = 50s$) with negligible transient response. When $t \in [20,50]s$, $\tilde{K}(\rho,[0,1])$ achieves smaller lateral error compared to $K_1(\rho)$ (see Fig. 11c), but with low steering noises as shown in Fig. 11d. Notice that these steering noises has been observed also in simulation section for $\tilde{K}(\rho,[0,1])$. When $t \in [65,85]s$, $\tilde{K}(\rho,[1,0])$ shows lower lateral error during maneuvering compared to $K_1(\rho)$. This appears since the LPV-YK controller $\tilde{K}(\rho,[1,0])$ is less conservative than the polytopic LPV controller $K_1(\rho)$.

8 Conclusion

This work has proposed a new YK-based method to: 1)Design several gain-scheduled controllers based on interpolation of previously designed LTI controllers at the vertices of the polytopic region; 2)Interpolate between them to obtain various performances. An external signal vector is introduced to the parameter region, which can be used to incorporate any ad-hoc

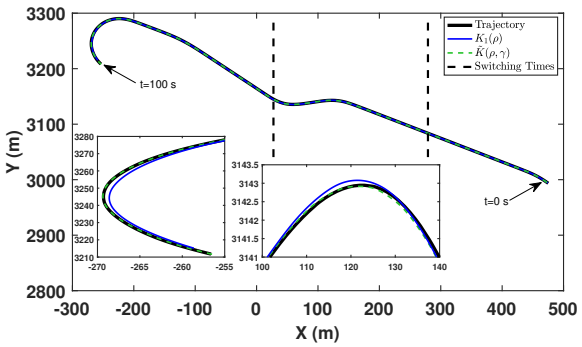

FIGURE 10 Experimental planned and controlled trajectories

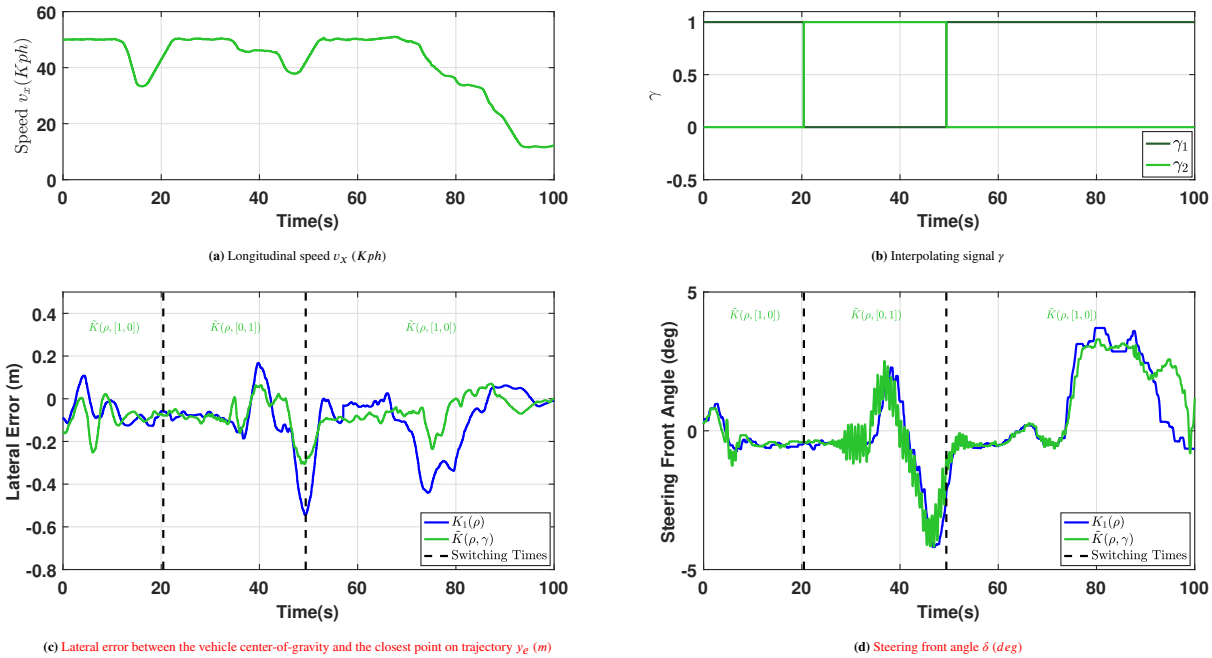

(a) Longitudinal speed v_X (Kph)

(b) Interpolating signal γ

(c) Lateral error between the vehicle center-of-gravity and the closest point on trajectory y_e (m)

(d) Steering front angle δ (deg)

FIGURE 11 Experimental results

physically-based interpolation, without adding any conservatism to the design problem. As a result, the closed-loop quadratic stability is guaranteed under arbitrary interpolating signal and arbitrary parameter-variations.

This approach improves the system performance, while dealing with various objectives and situations. An application to the autonomous vehicle lateral control is carried out. The simulation shows interesting results regarding the efficiency of the proposed method of providing high performance and ensuring safety at critical situations. In addition, experimental results are shown to validate its real performance by testing the approach on a real Renault ZOE vehicle.

Finally, notice that the LPV-YK control structure facilitates adding any new controller, by introducing its corresponding LPV-YK parameter to the YK configuration (as shown in Fig. 2), without recalling all the control design procedure. This enhances real applications, such as in industries, where the systems are subjected to frequent instrumentation changes such as autonomous vehicles. In addition, several applications can benefit from the proposed approach, specifically the ones that change dynamics or need to perform different closed-loop performances having wide range of parameter variations.

As future work, an interest appears to study the optimal choice of γ, and how to find always the best combination of a larger set of controllers, which will improve more the presented work.

References

1. Pacejka H. *Tire and vehicle dynamics*. Elsevier . 2005.

2. Rajamani R. *Vehicle dynamics and control*. New York, USA: Springer Science & Business Media . 2011.

3. Mariano R, Scalzi S, Netto M. Nested PID steering control for lane keeping in autonomous vehicles. *Control Engineering Practice* 2011; 19(12): pp 1459-1467. doi: 10.1016/j.conengprac.2011.08.005

4. Packard A. Gain scheduling via linear fractional transformations. *Systems & Control Letters* 1994; 22(2): 79-92. doi: https://doi.org/10.1016/0167-6911(94)90102-3

5. Rugh W, Shamma J. Research on Gain Scheduling. *Automatica* 2000; 36: 1401-1425. doi: 10.1016/S0005-1098(00)00058-3

6. Hoffmann C, Werner H. A Survey of Linear Parameter-Varying Control Applications Validated by Experiments or High-Fidelity Simulations. *IEEE Transactions on Control Systems Technology* 2015; 23(2): 416-433. doi: 10.1109/TCST.2014.2327584

7. Apkarian P, Gahinet P. A convex characterization of gain-scheduled H_∞ controllers. *IEEE Transactions on Automatic Control* 1995; 40(5): 853-864. doi: 10.1109/9.384219

8. Apkarian P, Gahinet P, Becker G. Self-scheduled H control of linear parameter-varying systems: a design example. *Automatica* 1995; 31(9): 1251–1261.

9. Fen Wu , Xin Hua Yang , Packard A, Becker G. Induced $\mathcal{L}_2$ norm control for LPV system with bounded parameter variation rates. In: . 3. ; 1995: 2379-2383 vol.3

10. Corno M, Panzani G, Roselli F, Giorelli M, Azzolini D, Savaresi SM. An LPV Approach to Autonomous Vehicle Path Tracking in the Presence of Steering Actuation Nonlinearities. *IEEE Transactions on Control Systems Technology* 2020: 1-9. doi: 10.1109/TCST.2020.3006123

11. Atoui H, Milanés V, Sename O, Martinez JJ. Design And Experimental Validation Of A Lateral LPV Control Of Autonomous Vehicles. In: ; 2020: 1-6

12. Atoui H, Sename O, Alcala E, Puig V. Parameter Varying Approach For A Combined (Kinematic + Dynamic) Model Of Autonomous Vehicles∗∗Institute of Engineering Univ. Grenoble Alpes. *IFAC-PapersOnLine* 2020; 53(2): 15071-15076. 21st IFAC World Congressdoi: https://doi.org/10.1016/j.ifacol.2020.12.2028

13. Lu B, Wu F. Switching LPV control designs using multiple parameter-dependent Lyapunov functions. *Automatica* 2004; 40: 1973-1980. doi: 10.1016/j.automatica.2004.06.011

14. Bianchi F, Peña R. Interpolation for gain-scheduled control with guarantees. *Automatica* 2011; 47(1): 239–243.

15. Niemann H. Dual Youla parameterisation. *IEE Proceedings - Control Theory and Applications* 2003; 150(5): 493-. doi: 10.1049/ip-cta:20030685

16. Rasmussen B, Chang Y. Stable Controller Interpolation and Controller Switching for LPV Systems. *Journal of Dynamic Systems Measurement and Control-transactions of The Asme - J DYN SYST MEAS CONTR* 2010; 132. doi: 10.1115/1.4000075

17. Blanchini F, Casagrande D, Miani S, Viaro U. Stable LPV Realization of Parametric Transfer Functions and Its Application to Gain-Scheduling Control Design. *IEEE Transactions on Automatic Control* 2010; 55(10): 2271-2281. doi: 10.1109/TAC.2010.2044259

18. Xie W, Eisaka T. Design of LPV control systems based on Youla parameterisation. *IEE Proceedings - Control Theory and Applications* 2004; 151(4): 465-472. doi: 10.1049/ip-cta:20040513

19. Hespanha J, Morse AS. Switching between stabilizing controllers. *Automatica* 2002; 38(11): 1905–1917.

20. Stoustrup J, Niemann H. Starting up unstable multivariable controllers safely. In: . 2. ; 1997: 1437-1438 vol.2.

21. Tay T, Moore J, Mareels I. *High performance control*. Springer Science & Business Media . 1997.

22. Stoustrup J. Plug&play control: Control technology towards new challenges. *European Journal of Control* 2009: 311-330.

23. Mahtout I, Navas F, Milanés V, Nashashibi F. Advances in Youla-Kucera parametrization: A Review. *Annual Reviews in Control* 2020. doi: 10.1016/j.arcontrol.2020.04.015

24. Landau I. On the use of Youla-Kucera parametrization in adaptive active noise and vibration control-A review. *International Journal of Control* 2018: 1-25. doi: 10.1080/00207179.2018.1548773

25. Mahtout I, Navas F, Gonzalez D, Milanes V, Nashashibi F. Youla-Kucera Based Lateral Controller for Autonomous Vehicle. In: ; 2018: 3281-3286

26. Bei Lu , Fen Wu , SungWan Kim . Switching LPV control of an F-16 aircraft via controller state reset. *IEEE Transactions on Control Systems Technology* 2006; 14(2): 267-277.

27. He T, Zhu G, Swei S. Smooth Switching LPV Dynamic Output-feedback Control. *International Journal of Control, Automation and Systems* 2019; 18. doi: 10.1007/s12555-019-0088-3

28. Hanifzadegan M, Nagamune R. Smooth switching LPV controller design for LPV systems. *Autom.* 2014; 50: 1481-1488.

29. Atoui H, Sename O, Milanes V, Martinez-Molina JJ. Toward switching/interpolating LPV control: A review. *Annual Reviews in Control* 2022; 54: 49-67. doi: https://doi.org/10.1016/j.arcontrol.2022.07.002

30. Atoui H, Sename O, Milanes V, Martinez JJ. LPV-Based Autonomous Vehicle Lateral Controllers: A Comparative Analysis. *IEEE Transactions on Intelligent Transportation Systems* 2021: 1–12. doi: 10.1109/tits.2021.3125771

31. Vidyasagar M. Control system synthesis: a factorization approach, part II. *Synthesis lectures on control and mechatronics* 2011; 2(1): 1–227.

32. Atoui H, Sename O, Milanes V, Martinez JJ. Interpolation of Multi-LPV Control Systems Based on Youla-Kucera Parameterization. under review in Automatica; 2021.

33. Angelis G. *System analysis, modelling and control with polytopic linear models*. PhD thesis. Department of Mechanical Engineering, 2001

34. Kosecka J, Blasi R, Taylor CJ, Malik J. Vision-based lateral control of vehicles. In: ; 1997: 900-905.

Author Biography

Hussam Atoui received his B.Sc. degree in Mechanical Engineering from Lebanese University, Beirut, Lebanon in 2019 and the M.Sc. degree in Automatic Control from Grenoble-Alpes University, Grenoble, France, in 2019. He is currently working toward the Ph.D. degree with Grenoble-Alpes University in a joint research between Gipsa-lab, Grenoble and Renault SAS, Guyancourt. His research interests concern switching control, youla parameterization, robust control, LPV control, and mainly control and motion planning of autonomous vehicles.

Olivier Sename received a Ph.D. degree from Ecole Centrale Nantes in 1994. He is now Professor at the Institut Polytechnique de Grenoble within GIPSA-lab. His main research interests include Linear Parameter Varying systems and automotive applications. He is the (co-)author of 2 books, 60 international journal papers, and more than 200 international conference papers. He was the General Chair of the IFAC Joint Conference SSSC-TDS-FDA 2013, of the 1st IFAC Workshop on Linear Parameter Varying Systems 2015 and he was the IPC Chair of the 2nd IFAC Workshop LPVS 2018. He has led several industrial (Renault, Volvo Trucks, JTEKT, Delphi) and international (Mexico, Italy, Hungary) collaboration projects. He has supervised 32 Ph.D. students.

Vicente Milanés received his Ph.D. degree in electronic engineering from University of Alcalá, Madrid, Spain, in 2010. He was with the AUTOPIA program at the Center for Automation and Robotics (UPM-CSIC, Spain) from 2006 to 2011. Then, he was awarded with a two-years Fulbright fellowship at California PATH, UC Berkeley. In 2014, he joined the RITS team at INRIA, France. Since 2016, he is with the Research Department at Renault, France. He is the author or a coauthor of more than 120 refereed publications in international journals, book chapters, and conference proceedings; and more than 10 industrial patents. His research interests cover multiple aspects in the autonomous vehicle field.

John J. Martinez was born in Cali, Colombia. He received the B.Sc. degree in electrical engineering and the M.Sc. degree in automatic control from the Universidad del Valle, Cali, in 1997 and 2000, respectively, and the Ph.D. degree in automatic control from the Institut National Polytechnique de Grenoble, Grenoble, France, in 2005. He joined the Universidad Nacional de Colombia, Medellin, Colombia, as a Teacher Assistant, from 2001 to 2002. He was an Invited Visitor with the Centre for Complex Dynamic Systems and Control, The Newcastle University, Callaghan, NSW, Australia, in 2005, 2007, and 2009. He is currently an associate professor at Grenoble-INP and researcher at GIPSA-lab (Control System Department). His research interest is related to modeling and robust control of mechatronic systems (e.g. Polytopic system modeling, Linear Parameter-Varying systems, Switching control and Invariant-Set Theory for Fault-Tolerant Control and Robust Disturbance Estimation/Rejection), mostly in the following applications: Automotive vehicle dynamics Safety, Aerial vehicle dynamics, Wind turbines control, Physiologic-aware electric bikes and Anti-vibration systems.